Environ Fluid Mech (2018) 18:985–1006
https://doi.org/10.1007/s10652-018-9585-9

ORIGINAL ARTICLE

Role of dispersed particles on the dynamics of an umbrella cloud of a forced plume in a linearly stratified environment

Sridhar Balasubramanian[1,2] · **Harish N. Mirajkar**[1] · **Ayan K. Banerjee**[1]

Received: 1 August 2017 / Accepted: 23 February 2018 / Published online: 6 March 2018

Abstract The vertical release of a lighter buoyant fluid, commonly referred to as a forced plume, into dense environment is a common occurrence in ocean and atmosphere. Such releases may have heterogeneity in them in form of particles with varied size, shape, and volume fraction. Normally in field conditions, the particle size ranges from a few microns to millimetres, and the volume fraction ranges from $\phi_v = 0.1-10\%$. In this study, the effects of low values of ϕ_v (corresponding to a two-way coupled system) on the dynamics and structure of a plume umbrella cloud formed in a linearly stratified ambient were examined. Spherical particles with mean diameter $d_p = 100\,\mu\text{m}$, density, $\rho_p = 2500\,\text{kg m}^{-3}$, and $\phi_v = 0-0.7\%$ were injected along with the lighter plume fluid. Due to the phenomena of "particle fall-out" and "particle re-entrainment", it was observed that a plume trough characterized by radius, R_c, and depth, L_p, forms below the neutral buoyant layer of an umbrella cloud. The plume trough formation is linked to the draw-down of the fluid from the neutral buoyant layer by the sedimenting particles. This trough either sustains or collapses depending on the plume conditions at the source, namely, the diameter d_0, fluid buoyancy, g_0', vertical velocity, W_0, and ϕ_v. In all the experiments, g_0' and d_0 were kept constant while $\phi_v = 0-0.7\%$ and $W_0 = 0.2-0.65\,\text{m s}^{-1}$ were varied. The experiments revealed that the sustaining and collapsing trough regimes could be qualitatively demarcated based on a source effective Richardson number, Ri_0^*, that accounts for the combined effect of ϕ_v and W_0. It was found that when $Ri_0^* < 0.018$, the plume trough collapses, otherwise it is sustained. However, Ri_0^* failed to predict the variations in R_c and L_p and hence was unsuitable for quantifying the plume trough. Therefore, it was established that the characteristics of a plume trough (i.e. R_c and L_p) depend independently on the particle volume fraction (ϕ_v) and source Richardson number (Ri_0), while the demarcation of the trough regimes could be done using Ri_0^*. For a constant $Ri_0 = \frac{-g_0' d_0}{W_0^2}$, with an

✉ Sridhar Balasubramanian
sridharb@iitb.ac.in

[1] Department of Mechanical Engineering, IIT Bombay, Mumbai, MH 400076, India

[2] Interdisciplinary Program in Climate Studies, IIT Bombay, Mumbai, MH 400076, India

increase in ϕ_v the trough radius, R_c, was found to decrease. In contrast, L_p increases for a sustaining trough and decreases for a collapsing trough. For a constant ϕ_v, a decrease in Ri_0 caused both R_c and L_p to increase irrespective of a sustaining or collapsing plume trough. Using equations of motion for sedimenting particles, an analytical expression for the trough radius, R_c, was formulated that accurately explains the experimental results. A relation for trough radius, R_c, that elucidates the dynamics of particle re-entrainment was also obtained. If a particle is within the value of R_c it is re-entrained into the plume, otherwise settles at the bottom. These results provide useful information needed for modeling particle-laden forced plumes.

Keywords Forced plume · Particles · Umbrella cloud · Richardson number · Plume trough

1 Introduction and previous work

In environmental and engineering fluid flows, the scalar transport of species commonly occurs in the form of a forced plume, where both momentum and buoyancy of the fluid control the plume dynamics. The release of hot gases during volcanic eruptions, gravity currents, fresh water overflow in ocean, and atmospheric pollutant dispersion are a few examples. It is natural for forced plumes to have particles in them (as a dispersed phase) that may modify their flow behaviour. Therefore, for a forced plume-like flow, in addition to momentum and buoyancy, the particle volume fraction, ϕ_v, is an additional parameter governing the flow physics. It is therefore imperative to quantify the effects of solid particulate-phase on plume evolution, growth, entrainment, and its structure to accurately model its dynamics. When a forced plume, without any particles (i.e. a single-phase forced plume), is released into a linearly stratified atmosphere, momentum and buoyancy cause it to move upwards. As it moves up, it entrains the denser fluid from the surroundings by the process of turbulent exchange. This entrainment produces a radial inward velocity field in the surroundings due to which the plume loses its buoyancy, becomes neutrally buoyant, and forms an umbrella cloud as the plume starts spreading radially out as a gravity current. The height where this happens is termed as the "spreading height" denoted by Z_s [20]. If particles are present (multi-phase forced plume), they will sediment from the cloud and may get re-entrained into the rising plume [6, 13, 18, 27, 29]. The purpose of this study is to examine the effects of sedimentation and re-entrainment on the large-scale characteristics of a forced plume in a linearly stratified environment.

Even though forced plumes have been a topic of research for long, ever since the pioneering work of Morton et al. [20], only a handful of studies have explored the effect of particles on their dynamics. For a single-phase forced plume, Morton et al. [20] provided the entrainment assumption and first set of equations for volume flux, $V(z)$, momentum flux, $M(z)$, and buoyancy flux, $B(z)$, using the plume width, $b(z)$, and the vertical velocity of the plume $W(z)$, with z being the vertical distance. The work was later extended by [19] for a forced plume with non-zero values of source volume flux (V_0), source momentum flux (M_0), and source buoyancy flux (B_0). In particular, the source momentum flux, M_0, and source buoyancy flux, B_0, are found using

$$M_0 = V_0 W_0 \tag{1}$$

$$B_0 = -g\left(\frac{\rho_{01} - \rho_0}{\rho_0}\right)V_0 = -g_0' V_0 \tag{2}$$

where $V_0 = \frac{1}{4}\pi d_0^2 W_0, d_0$ is the diameter of the plume source, g_0' is the buoyancy at the source, W_0 is the source velocity, ρ_0 is the density of the ambient fluid at the source, and ρ_{01} is the density of the plume fluid at the source. Interestingly, for particle-laden forced plumes another kind of buoyancy flux at the source could be defined, called the source effective buoyancy flux, B_{0eff}, which takes the form

$$B_{0eff} = -g\left(\frac{\rho_{0eff} - \rho_0}{\rho_0}\right)V_0 = -g_{0eff}' V_0 \tag{3}$$

Here g_{0eff}' is the effective buoyancy at the source and ρ_{0eff} is the effective density of the fluid at the source, which takes into account the density of the plume fluid and the particle. It is given by $\rho_{0eff} = \phi_f \rho_{01} + \phi_v \rho_p$, with ϕ_f=1-ϕ_v. Effective buoyancy and fluid buoyancy are related to each other as $g_{0eff}' = g_0' - \frac{g\phi_v(\rho_{01}-\rho_p)}{\rho_0}$.

Turner [28] stated that for a forced plume, the jet-like region is quite small and it behaves as a buoyancy dominated flow since the initial momentum is increased by buoyancy. The buoyancy generated momentum dominates above a height of the order $l_M = \frac{M_0^{3/4}}{B_0^{1/2}}$ [19]. Papanicolaou and List [22] showed that the dimensionless distance, $\frac{z}{l_M}$, from the flow source has to vary from very small in jets to over 5 in plumes. They stated that $1 < \frac{z}{l_M} < 5$ for a forced plume, $\frac{z}{l_M} > 5$ for a pure plume, and $\frac{z}{l_M} < 1$ for a jet. Using scaling arguments, Hunt and Kaye [14] suggested that based on the balance of momentum flux, buoyancy flux, and volume flux at the plume source, different flow regimes for a single-phase plume could be defined using a parameter $\Gamma_0 = \frac{5V_0^2 B_0}{4\alpha M_0^{5/2}}$, where α is the entrainment coefficient, which takes a value $\alpha = 0.068$ corresponding to the forced plume case [18]. Balancing the fluxes at the source, the classifications are as follows: lazy plume ($\Gamma_0 > 1$), pure plume ($\Gamma_0 = 1$), and forced plume ($\Gamma_0 < 1$). In a physical sense, a lazy plume arises from a source with a deficit of momentum flux compared to a forced plume with the same source buoyancy and volume fluxes. Wong and Wright [31] and Bloomfield and Kerr [4] introduced a non-dimensional parameter $\sigma = \frac{M_0^2 N^2}{B_0^3}$ to distinguish the flow taking into account the effect of stratification, $N = (-\frac{gd\rho}{\rho_0 dz})^{1/2}$. When $\sigma \gg 1$ represents strong stratification and/or high velocity and/or a low density deficit, with the converse true for $\sigma \ll 1$. It has been widely accepted that $\sigma^{1/2}$ is a measure that controls the plume rise height in a linearly stratified fluid [23]. The experiments by Bloomfield and Kerr [4] on fountains in uniform stratification provided good semi-empirical predictions of the spread height based on the dimensionless parameter $\sigma^{1/2}$. It was proposed by them that

$$Z_s = 2.5\left(\frac{B_0}{N^3}\right)^{1/4}, \quad \sigma^{1/2} = \frac{MN}{B} < 1$$

$$Z_s = 1.5\left(\frac{M_0}{N^2}\right)^{1/4}, \quad \sigma^{1/2} = \frac{MN}{B} > 10$$

Richards et al. [23] performed experiments on forced plume in uniform stratification to overcome the limitations of experiments by [4], where momentum and buoyancy had

different signs. This allowed Richards et al. [23] to study the intrusions from buoyancy dominated as well as momentum dominated source conditions. They again used $\sigma^{1/2}$ to parameterize the spreading height and showed that the relation $Z_s = 2.5(\frac{B_0}{N^3})^{1/4}$ is valid for $\sigma^{1/2} = \frac{MN}{B} \leq 7$. Therefore, this parameterization for Z_s can be applied to a forced plume, which is dominated primarily by buoyancy (since $\sigma^{1/2}$ is small and the flow is plume-like and driven by buoyancy). In fact, recent studies have used this parameterization for Z_s for a forced plume and shown that it matches experimental results [17, 18, 23]. For $\sigma^{1/2} > 7$, the flow is dominated by momentum and is closer to a jet-like flow. In the present study, our focus is primarily on forced plumes that are dominated by buoyancy, for which $\sigma^{1/2} < 7$. The value of $\frac{Z_s}{l_M}$ for our experimental conditions lies between $1 < \frac{Z_s}{l_M} < 5$, which corresponds to a forced plume.

Moving on to studies on plume dynamics in the presence of particles, pioneering work on particle-laden plumes was done by Carey et al. [8] who studied plumes released in dense stratified environment. For particle plumes, additional parameters in the form of settling velocity, w_s, and particle volume fraction, ϕ_v, are introduced. In Carey et al. [8], the continuous plume phase was positively buoyant but contained negatively buoyant particles. The effect of varying volume fraction on the stability of the plume and particle distribution was documented. Leah [16] studied particle-laden plume in linearly stratified medium to model the bubble plume for varying particle diameter and determined the maximum height of the plume (Z_M). Sparks et al. [26] and German and Sparks [13] studied sedimentation from intruding gravity currents generated by turbulent plumes in unstratified environment. They proposed a critical radius for particle re-entrainment into the plume based on the motion of sedimenting particles. The critical radius was defined as the distance where the particles separating out from the intruding fluid could be re-entrained back into the plume. Woods [32] studied the dynamics of particle-laden plumes using steady models averaged over the timescale of turbulent fluctuations but neglected the effects of particle recycling. German and Sparks [13] and Veitch and Woods [29] reported that particle recycling may have a significant effect on the dynamics of a forced plume and independently reported the effect of particle recycling on the dynamics of a plume, critical radius for re-entrainment, and collapse criteria in unstratified fluids. Veitch and Woods [29] also showed that as particles began to settle through the ambient fluid, they draw-down the plume fluid from the neutral layer and form a distinct plume collar below it. As the particle volume fraction was increased, the downward motion of the particle was vigorous, drawing down a substantial part of the plume fluid from the neutral layer and triggering partial or total collapse. The reason for collapse was attributed to the gradually re-entrained particles into the plume, decreasing its buoyancy, until eventually, the plume ceased to be buoyant and collapsed upon itself. It is important to remember that the work by German and Sparks [13] and Veitch and Woods [29] are for particle-laden plumes in unstratified fluids. Chan [9], Chow [10] and Socolofsky and Adams [25] observed the dynamics of a positively forced plume with positively buoyant particles (in form of oil droplets/bubbles). They reported intrusion and peeling of the plume at different levels depending on the particle volume fraction. An integral based approach was also reported to model the intrusions. Their study is very different from ours where the plume is positively buoyant but the particles are negatively buoyant. Our results are significantly different from those of Socolofsky and Adams [25] and the differences are elaborated in section 4.3.

Recently, Carazzo and Jellinek [6] studied the particle plume stability in a step stratification configuration. They reported evidence of finger-like structures (similar to plume

collar reported by [29]) beneath the neutral layer for some values of ϕ_v and collapse of the fingers like structure as ϕ_v was increased. They also found a value of source effective Richardson number, $Ri_0^* = \frac{-g'_{0eff} d_0}{W_0^2}$, at which the fingering instability below the umbrella cloud caused the plume to collapse. However, the values of particle diameter and volume fraction used were much higher than that reported in the present study. A major difference between their study and ours is that they considered the plume fluid to be denser than the ambient, thereby allowing the plume to behave like a fountain, wherein the source momentum and source buoyancy have opposite signs. In our study, the source momentum and buoyancy have the same sign. In the studies by Veitch and Woods [29] and Carazzo and Jellinek [6], the plume collar was not at all characterized quantitatively. Jessop and Jellinek [15] studied the effect of particles on the umbrella cloud and found that the effect of particles modified the dynamics, stability and longevity of the umbrella clouds. However, no quantitative analysis was done and a step stratified fluid layer was used in their study. Mirajkar et al. [18] observed the effects of low concentration of particles on the dynamics of a plume evolving in a linearly stratified environment. They observed the formation of a plume trough below the neutral layer and its collapse due to the presence of negatively buoyant particles. The plume trough is analogous to a plume collar or the finger-like structures observed by other researchers. Mirajkar et al. [18] too attributed the formation of this plume trough to the dragging down of the fluid due to particle sedimentation and re-entrainment. Further, it was observed that the radial intrusion was slower for a particle-laden plume compared to single-phase plumes. Recently Sutherland and Hong [27] studied the structure of the settled particle mound and found that its variation as a function of radius can be represented by a Gaussian function. Apart from the above studies, effects of dispersed particles on plume dynamics and turbulence modulation in homogeneous fluid have been studied by various researchers [1, 3, 7, 11, 12]. It was concluded that the flow characteristics are modified even at very low particle concentrations, and hence should be appropriately modeled. At low particle concentrations, the two-way coupling mechanism is dominant, which is the primary reason for choosing the range of particle volume fractions, ϕ_v explored in our study.

Based on the review of past literature on particle-laden plumes, the following gaps on this topic have been identified, which are addressed in our study to improve the understanding and modeling of such plumes: (1) the structure (i.e. depth and radius) of the plume trough has not been characterized. The quantification of plume trough is important since it is a stand-out feature of particle-laden plumes, which influences the entrainment and flow dynamics. In our earlier paper on particle-laden plumes [18], the plume trough was qualitatively observed but not characterized. A plume trough can be precisely quantified by measuring the radial spread and depth of the dragged fluid from the neutral buoyant layer. (2) The effects of particle volume fraction, ϕ_v, and source Richardson number, Ri_0, on the plume trough have not been quantified. (3) Lastly, past studies have considered either unstratified or step-stratified ambient. Therefore, the effect of linearly stratified ambient on the evolution of a particle-laden plume has not been documented. Specifically, we report experiments performed to quantify the plume trough depth, L_p, and trough radius, R_c, and their sensitiveness to variations in ϕ_v and Ri_0. Additionally, theoretical formulations are presented to validate some of the experimental measurements.

In the present study, $\Gamma_0 < 1$ and $0.5 < \sigma^{1/2} < 3$ in all our experiments (shown in Table 1 below). This indicates that we are dealing with a forced plume and its dynamics. In the subsequent sections, the terminologies "plume" or "forced plume" have the same connotation.

Table 1 Source parameters in the experiments

Run no.	d_0 (cm)	N (s $^{-1}$)	W_0 (cm/s)	Re_0	B_0 (m ^{4}/ s ^{3}) x10^{-6}	M_0 (m ^{4}/ s ^{2}) $\times 10^{-6}$	Γ_0	Ri_0	$\sigma^{1/2}$
1	1.27	0.67	26.0	3670	5.31	8.56	0.42	0.030	1.09
2	1.27	0.67	19.7	2780	4.02	4.91	0.73	0.052	0.83
3	1.27	0.67	26.0	3670	5.31	8.56	0.42	0.030	1.09
4	1.27	0.67	26.0	3670	5.31	8.56	0.42	0.030	1.09
5	1.27	0.67	26.0	3670	5.31	8.56	0.42	0.030	1.09
6	1.27	0.67	26.0	3670	5.31	8.56	0.42	0.030	1.09
7	1.27	0.67	40.0	5560	8.04	19.6	0.19	0.013	1.68
8	1.27	0.67	52.0	7330	10.6	34.2	0.10	0.007	2.18
9	1.27	0.67	52.0	7330	10.6	34.2	0.10	0.007	2.18
10	1.27	0.67	52.0	7330	10.6	34.2	0.10	0.007	2.18
11	1.27	0.67	65.0	9170	13.2	53.5	0.07	0.004	2.73

2 A note on particle-laden plumes

A fundamental dimensional analysis for plumes reveals that any external parameter, say A, can be written as a function of all the governing properties as follows,

$$A = f\left(W_0, d_0, g_0', w_s, N, \phi_v\right)$$

Using Buckingham Π theorem, we can write the above equation in non-dimensional form as,

$$A^* = F\left(Ri_0, \frac{w_s}{W_0}, \phi_v, \frac{Nd_0}{W_0}\right)$$

where $Ri_0 = \frac{-g_0' d_0}{W_0^2}$ is the source Richardson number which shows the relative effect of buoyancy and momentum. In this work, since we are dealing with forced plumes, the source momentum will be higher than the source buoyancy thereby giving low values of $Ri_0 (Ri_0 = 0.004{-}0.013)$. However, as stated before, the jet-like region would be small and the evolving flow will behave as a plume above a height given by $l_M = \frac{M_0^{3/4}}{B_0^{1/4}}$ [28]. From the above relation, we see that for single-phase plumes, the factor that affects the plume dynamics is Ri_0 and $\frac{Nd_0}{W_0}$. Combining Ri_0 and $\frac{Nd_0}{W_0}$, such that $(\frac{Nd_0}{W_0})/(Ri_0)$, we realize that it is same as the parameter $\sigma^{1/2}$ used for study of single-phase plumes. Since, the stratification strength is constant in the present study, the only governing parameter becomes Ri_0. The use of bulk Richardson number, Ri_0, for quantifying dynamics of single-phase plumes in stratified environments is reported in other studies as well [24, 30].

In the presence of particles, we have extra governing parameters in the form of $\frac{w_s}{W_0}, \phi_v$. Since the particle inertia is much smaller than the fluid inertia at the source, $\frac{w_s}{W_0}$ can be ignored. Therefore, for particle-laden plumes with constant value of N, we get,

$$A^* = F(Ri_0, \phi_v) \tag{4}$$

Therefore, the variation of any external parameter A^* could be studied independently with Ri_0 and ϕ_v. In the present work, we mainly focus on the effect of particle volume fraction and source fluxes on the plume dynamics. The future work can explore the effect of varying N on the dynamics of the plume trough.

Carazzo and Jellinek [6] proposed a modified Richardson number formula by introducing the effective buoyancy, g'_{0eff} (defined in Sect. 1), to account for the particle density and volume fraction. Thus, an effective source Richardson number Ri_0^* could be formulated that takes the form

$$Ri_0^* = \frac{-g'_{0eff} d_0}{W_0^2} \tag{5}$$

It is important to note that Ri_0^* doesn't come up in the dimensional analysis and is based on empiricism, which accounts for change in the buoyancy due to the presence of particles. For the case of particle-laden plume with negatively buoyant particles, keeping the source buoyancy, g'_0, constant one could still change g'_{0eff} by changing the value of ϕ_v. For instance, assume that g'_0 is constant, but ϕ_v and W_0 are varying, such that $(\phi_v)_{case1} < (\phi_v)_{case2}$ and $(W_0)_{case1} > (W_0)_{case2}$. Here, $(Ri_0)_{case1} < (Ri_0)_{case2}$, implying case 1 has relatively higher initial momentum than case 2. However, Ri_0^* depicts a completely different picture, where depending on ϕ_v, both the cases can have the same Ri_0^* but completely different flow dynamics. As an illustration (reference to Table 2 below), for the d_p and ρ_p of particles used in our experiments, if $g'_0 = 0.16\,\mathrm{m\,s^{-2}}, Ri_0^*$ is same in both the cases when (a) $\phi_v = 0.5\%$ and $W_0 = 0.65\,\mathrm{m\,s^{-1}}$ and (b) $\phi_v = 0.7\%$ and $W_0 = 0.52\,\mathrm{m\,s^{-1}}$. Comparing the two cases, due to a significant "particle fall-out" effect (owing to a higher value of ϕ_v, see [18]) in (b) the plume dynamics and the structure of the plume trough would be very different. Therefore, it is obvious that the variations in L_p and R_c of the plume trough cannot be quantified using the effective Richardson number, Ri_0^*. In view of this, the variations in L_p and R_c have to be studied independently with ϕ_v and Ri_0.

Table 2 Plume trough regimes observed in the experiments

Run no.	d_0 (cm)	N (s $^{-1}$)	W_0 (cm/s)	d_p (μm)	ϕ_v (%)	Ri_0	Ri_0^*	Regime
1	1.27	0.67	26.0	100	0	0.030	0.030	No trough
2	1.27	0.67	19.7	100	0.50	0.052	0.029	Sustaining trough
3	1.27	0.67	26.0	100	0.35	0.030	0.020	Sustaining trough
4	1.27	0.67	26.0	100	0.45	0.030	0.018	Sustaining trough
5	1.27	0.67	26.0	100	0.50	0.030	0.017	Collapsing trough
6	1.27	0.67	26.0	100	0.70	0.030	0.011	Collapsing trough
7	1.27	0.67	40.0	100	0.50	0.013	0.007	Collapsing trough
8	1.27	0.67	52.0	100	0.35	0.007	0.005	Collapsing trough
9	1.27	0.67	52.0	100	0.50	0.007	0.004	Collapsing trough
10	1.27	0.67	52.0	100	0.70	0.007	0.003	Collapsing trough
11	1.27	0.67	65.0	100	0.50	0.004	0.003	Collapsing trough

Carazzo and Jellinek [6] used an effective source Richardson number Ri_0^* solely to demarcate the stable and collapsing regimes of the finger-like structures encountered in their study. They didn't quantify the structure of this finger-like structure, which is similar to the plume trough seen in our study. Therefore, we conclude that Ri_0^* is a suitable parameter to qualitatively distinguish stable and collapsing plume trough and we solely use it for this purpose in the present study.

3 Experimental set up and flow conditions

The experimental setup, shown in Fig. 1a, primarily consists of two acrylic tanks, one used for storing the plume fluid and the other for storing the ambient fluid [17]. The tank (T1) comprised of the plume fluid, a dye mixed with water of density $\rho_1 = 999.3\,\mathrm{kg/m^3}$. The second tank (T2) was used for storing the ambient linearly stratified fluid. The tank was linearly stratified using aqueous NaCl solution by using double bucket technique as discussed in Oster and Yamamoto [21]. The vertical density profile was measured with the help of a Delta-Ohm conductivity probe and the profile was found to be linear with an error of $\pm 2\%$ (see Fig. 1b). The stratification strength was kept constant in all the experiments with a value of $N = 0.67\ \mathrm{s}^{-1}$. It is possible to get same values of Ri_0 (as those mentioned in the experiments) by changing the value of N but keeping the velocity (W_0) constant. For a given Ri_0, irrespective of whether N or W_0 is changing, the plume dynamics will remain the same.

At the start of any given experiment, a centrifugal pump was used to discharge the plume fluid from T1 into the ambient linearly stratified environment, T2, using a round nozzle, with diameter $d_0 = 1.27$ cm, seated at the bottom of the tank. The volume flow rate, V_0, controlled by a needle valve and measured using an electromagnetic flowmeter, was maintained constant during each experimental run. However, V_0 was varied between $V_0 = 2.5$ to $8.2 \times 10^{-5}\,\mathrm{m^3\,s^{-1}}$ from one set of experiments to the other. The plume fluid injection lasted $t = 240\,\mathrm{s}$ and the plume evolution was recorded using a digital camera. During this period, it was confirmed that the plume radial propagation and plume trough development were devoid of any sidewall effects. Experiments were conducted by varying both the source Richardson number, Ri_0, and particle volume fraction, ϕ_v. The parameter

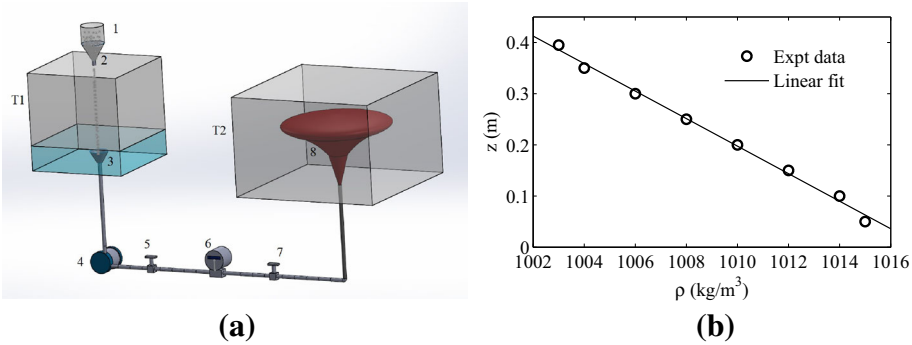

Fig. 1 **a** Schematic of the experimental setup. 1. Conical particle feeder, 2, 5, 7. Control valve, 3. Funnel, 4. Centrifugal pump, 6. Electromagnetic flowmeter, 8. Umbrella cloud formation. In the figure, $T1$ is the plume fluid tank, and $T2$ is the stratification tank. **b** Density profile in the experiments

range covered in this study is presented in Table 1. The source Reynolds number is defined as $Re_0 = \frac{W_0 d_0}{\nu}$ and the values show that the plume is turbulent at the source. It is noted that Re_0 for volcanic eruptions vary in the range $10^7 \leq Re_0 \leq 10^9$, which is difficult to simulate at the laboratory scale. Our flows are at considerably high Reynolds number, fully turbulent and conducted under conditions comparable to previous studies on this topic [5]. Five different values of source Richardson number were used, $Ri_0 = 0.052, 0.030, 0.013, 0.007, 0.004$. The lowest values of Ri_0 indicate high momentum flow and the highest value of Ri_0 indicates low momentum flow. Four different particle volume fractions were used, $\phi_v = 0, 0.35, 0.45, 0.5$ and 0.7%. The value of ϕ_v was deliberately kept at $\phi_v < 1\%$ to ensure that the two-way coupling regime is dominant [3]. In the presence of particles, the density ratio $\Delta\rho = \frac{\rho_0 - \rho_{0eff}}{\rho_0} < 2\%$ and hence the flow is in the limit of Boussinesq approximation [2].

Each experimental run was repeated five times to obtain statistically averaged data. The variations between the repeated runs were quantified using the maximum height, Z_m and spreading height, Z_s of the plume. It was seen that the variations in Z_m and Z_s were within $\pm 2\%$, rendering the experiments highly repeatable (see [18]). Proper care was taken to ensure that the variation in the particle volume fraction, ϕ_v, between the repeated runs was negligible. This was done by collecting the particles on an Aluminum plate kept at the bottom of the tank, followed by drying and weighing after end of every run. The flow dynamics were captured using a commercial dye solution with the help of a high resolution digital camera. Two cameras, one from the top and one from the side, were fitted to record the flow dynamics in the $r-z$ plane (front view) and $r-\theta$ plane (top view). While the images from the front camera were used to measure plume evolution and formation of the trough, the top camera was installed to check the plume's symmetry, which was confirmed from the images. The spatial resolution of the two cameras were fixed at 0.625 mm/pixel. A lighting arrangement was made around the tank to ensure that the background was similar for all the experiments. Characteristics of the plume trough were found using an intensity threshold algorithm followed by edge detection in MATLAB. The images obtained from the camera were converted to binary form by applying a threshold cut-off of $\approx 10\%$ of the maximum intensity value. The threshold helps in differentiating the plume from the background. Since, the binary image is in black and white form, the detection of boundary of the plume becomes trivial, which would give us information about the plume structure below the neutral layer. It was also checked that maintaining a cut-off value between 5 and 10% of the maximum intensity gave a good estimate of the plume boundary, which was within the experimental error limit. Based on this sensitivity analysis, the intensity cut-off value was fixed at $\approx 10\%$ of its maximum value. The uncertainty involved with the intensity threshold analysis was found to be within $\pm 2\%$. Since the pixel values are converted to physical units (e.g. depth of the plume trough in cm), the uncertainty in measurement of L_p and R_c is also $\pm 2\%$.

A detailed investigation on the structure of the plume trough formed in a particle-laden forced plume was carried out. A theoretical analysis was also carried out to corroborate the experimental results. The results are divided into two sections, namely, the effect of volume fraction on plume trough, and the effect of source Richardson number on plume trough. A mathematical model is developed based on equations of motion for sedimenting particles to validate the experimental measurements.

4 Results and discussion

4.1 Effect of particle volume fraction on the structure of plume trough

As a forced particle-laden plume reaches the neutral buoyant layer, it starts to spread radially outward forming an umbrella cloud. In the presence of particles, due to the downward settling velocity of the particles and horizontal entrainment velocity of the plume, a distinct trough is formed (see Fig. 2), which is unique to particle-laden plumes [18]. Such a trough below the neutral spreading height is absent in single-phase plumes. The formation of this trough is associated with the two-way coupling interaction between the fluid and particles. To elaborate the mechanism of the trough formation, as the lighter plume fluid rises up, it reaches the neutral buoyant layer and starts spreading radially. The particles start sedimenting, due to the "particle fall-out" phenomenon [18], and in the process drag down the plume fluid from the neutral layer along with it. Simultaneously, the particles could also radially move-out or into the plume due to re-entrainment. This downward and radial outward/inward motion of the particles results in the formation of a plume trough. Depending on the value of ϕ_v, the trough either reaches a steady state (sustains itself) or continuously grows until it reaches the source (collapses). The sustenance and collapse of the plume trough can be explained using the re-entrainment of particles into the plume. It has been shown in unstratified environment that a trough radius, R_c, exists and if the particle is within this R_c, then it is re-entrained into the plume fluid, otherwise settles on the bottom [26]. If the particle is re-entrained, then in the presence of particles (heavier than the fluid), the fluid buoyancy is drastically reduced, thereby inhibiting its rising motion and resulting in the collapse of the trough. On the other hand, for some values of ϕ_v, the particles re-entrainment and recycling into the plume are not sufficient to reduce the buoyancy flux thereby stabilizing the plume trough. Hence, it is important to characterize the structure of the plume trough to in response to varying values of ϕ_v. The structure of the plume trough is characterized by its depth, L_p, and radius, R_c, shown schematically in Fig. 3. It should be noted here that the depth and radius of the trough can be measured by looking only at the expanse of the dyed fluid in the experiments. There is no need to track the particle-motion since the trough is defined as the amount of the plume fluid dragged from the neutral layer. The two-way coupling interaction ensures that the fluid and particles and coupled together and the bulk motion of the particles is represented in the fluid motion.

Depending on the value of ϕ_v, the trough either reaches a steady state or continuously grows until it reaches the source. The depth of this trough, L_p, can be defined as the vertical

Fig. 2 Image of the plume trough formation below the umbrella cloud at time $t = 120$ s, $\phi_v = 0.5\%, Ri_0 = 0.030$

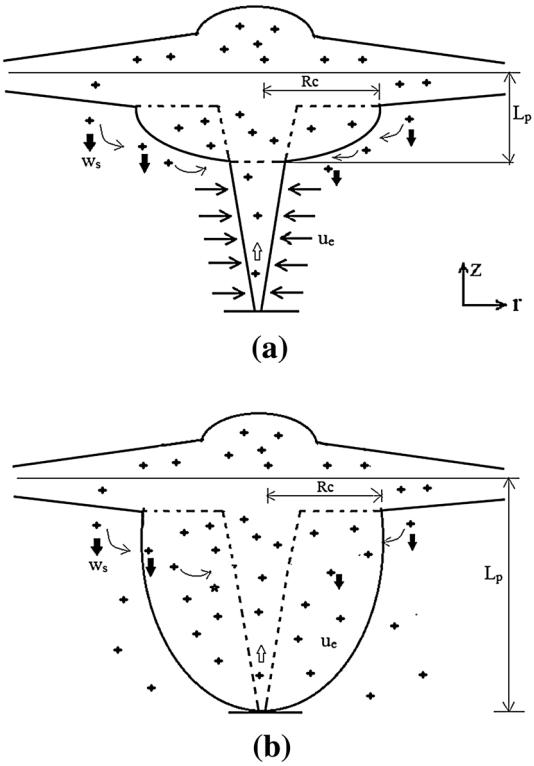

Fig. 3 Schematic of the plume trough depicting the depth and radius of the trough **a** for a sustaining plume trough and **b** for a collapsing plume trough

distance of the dragged fluid from the neutral buoyant layer. If the trough reaches the source, we tag it as "collapse" of the trough and the definition of L_p becomes same as Z_s. Similar collapse phenomenon was also observed by Carazzo and Jellinek [6] where much higher values of ϕ_v were used. The evolution and collapse of the trough for the different time intervals is shown in Fig. 4 for a constant value of $Ri_0 = 0.030$. It was observed that with increase in the volume fraction of particles, the trough increased with time. For single-phase plume, where $\phi_v = 0\%$, a trough formation was not observed. When $\phi_v \leq 0.45\%$, the plume trough was seen to sustain itself. For high values of $\phi_v = 0.5$ and 0.7%, the plume trough collapses and reaches the source. Interestingly, during the collapse, the particles are re-entrained into the plume leading to the formation of a secondary structure, which we call "secondary umbrella cloud". The formation of a secondary umbrella cloud was weakly observed for $\phi_v = 0.5\%$, and very distinctly for $\phi_v = 0.7\%$. The quantification of the structure of a secondary umbrella cloud is presently out of purview of this work.

Here it is imperative to demarcate the steady and unsteady regimes during plume evolution, since the dynamics of particle-laden plumes are complex. It is seen from Fig. 4 that a plume behaves differently depending on the particle volume fraction (ϕ_v). For instance, comparing $\phi_v = 0.45\%$ and 0.5%, at two different times (say $t = 80$ s and $t = 150$s), the umbrella cloud does not collapse for the case of $\phi_v = 0.45\%$, but collapses for $\phi_v = 0.5\%$. In fact, for $\phi_v = 0.45\%$, the umbrella cloud does not collapse for even at $t = 200$ s. This points to the fact that based on the amount of particles, a plume may attain a steady-state behaviour with a sustained trough or an unsteady behaviour with collapse of

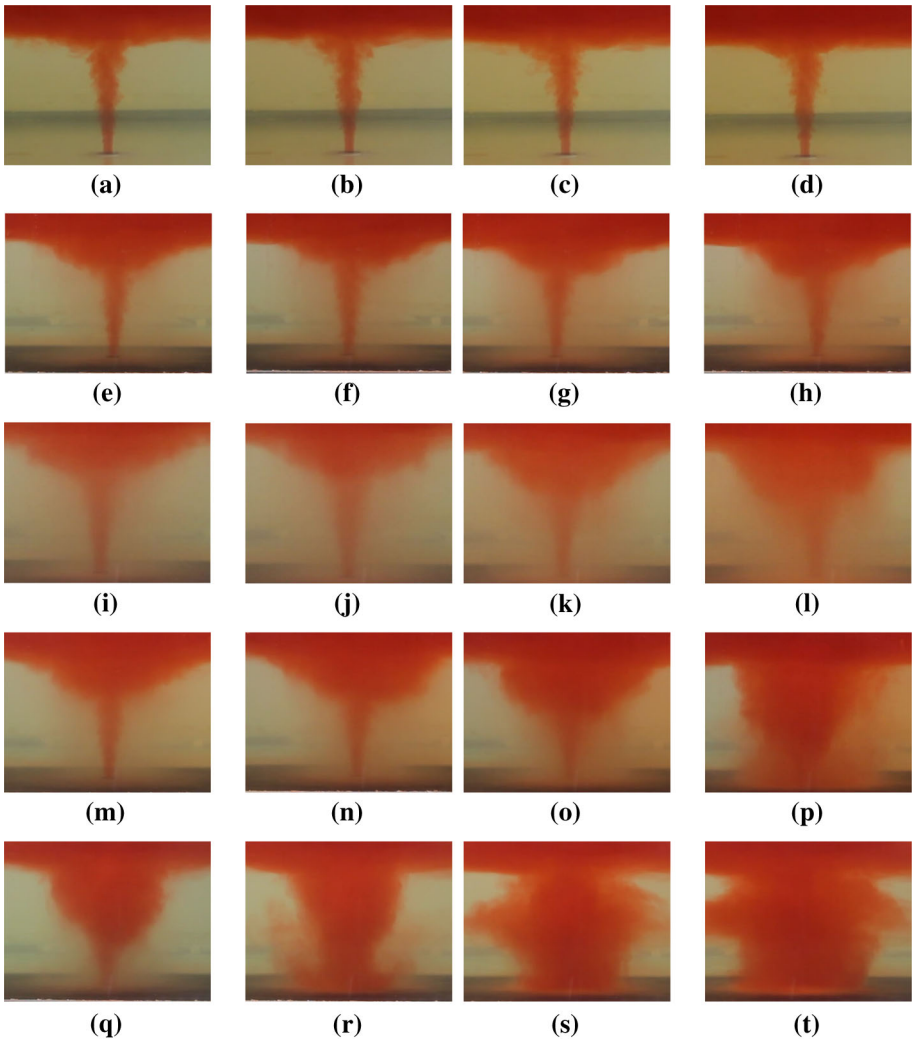

Fig. 4 Evolution and collapse of the trough below the umbrella cloud for different time intervals **a** $t = 40$ s, **b** $t = 80$ s, **c** $t = 120$ s, **d** $t = 150$ s, **a–d** single phase plume, $\phi_v = 0\%$, **e–h** $\phi_v = 0.35\%$, **i–l** $\phi_v = 0.45\%$, **m–p** $\phi_v = 0.5\%$, **q–t** $\phi_v = 0.7\%$. The source Richardson number is $Ri_0 = 0.030$

the trough. This is primarily due to the plume-particle interaction, which allows demarcation of the plume evolution based on the particle volume fraction (ϕ_v).

For different ϕ_v values at a constant $Ri_0 = 0.030$, the growth of the trough depth, L_p with time is shown in Fig. 5a and the variation of L_p as a function of ϕ_v is plotted in Fig. 5b. It should be noted that in Fig. 5b, the last value of L_p from Fig. 5a is plotted. For low values of ϕ_v, the trough depth L_p increases with increasing ϕ_v. It is seen that the growth of L_p is inhibited when $\phi_v > 0.5\%$, reflecting the plume collapse phenomenon, which is not seen when $\phi_v < 0.5\%$. This observation is inline with that of Fig. 4, where the plume never collapses for a lower values of ϕ_v for the entire duration of the experiment, indicating a steady state trough without any possibility of collapse. The physical

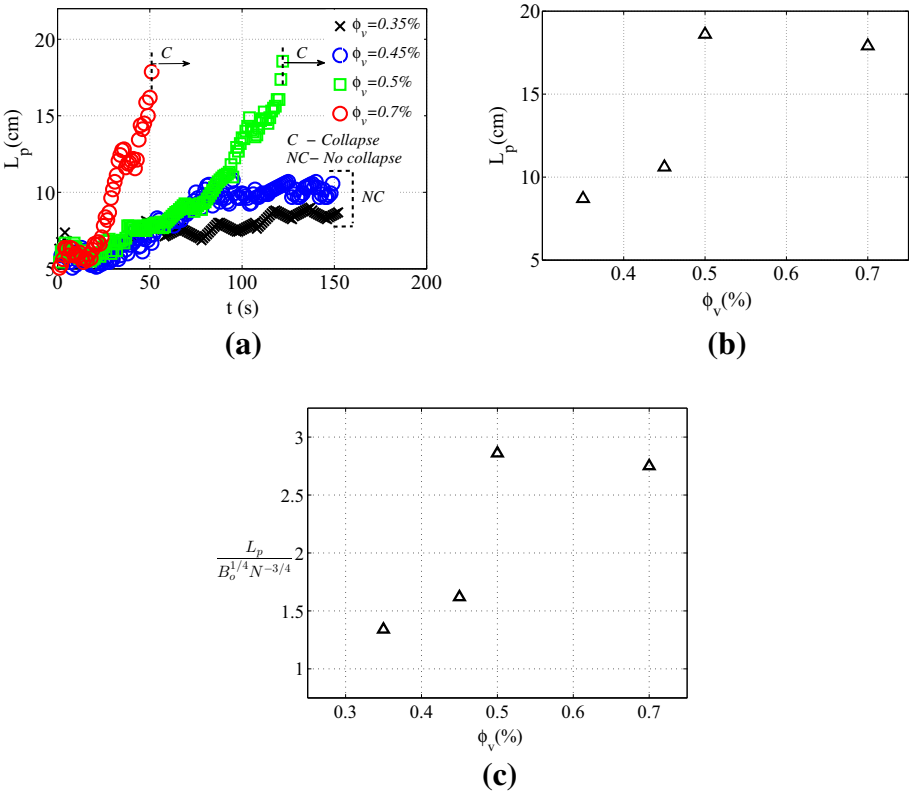

Fig. 5 **a**, **b** Trough depth L_p for the different particle volume fraction, ϕ_v, at $Ri_0 = 0.030$, **c** normalized plot of trough depth with the volume fraction, ϕ_v

explanation for such a trend in L_p is as follows: For a sustained plume trough (i.e. for values of $\phi_v < 0.5\%$), when all other source conditions are maintained constant, an increase in the particle volume fraction, ϕ_v energizes the "particle fall-out" phenomenon [18]. The falling particles drag the plume fluid along with it leading to higher values of L_p. As ϕ_v is increased beyond 0.5%, it triggers a collapse of the trough, thus reversing the trend of L_p (seen in Fig. 5b). Now, for a collapsed plume trough $L_p = Z_s$. Mirajkar et al. [18] documented that as ϕ_v increases the spreading height Z_s decreases. Hence, for values of ϕ_v triggering plume collapse, L_p shows a decreasing trend with increase in particle volume fraction. The variation of L_p (vs) ϕ_v at a different value of Ri_0 showed a similar trend. Hence, we only present in detail the results for one such $Ri_0 (= 0.030)$ and note that the dynamics are same for other values as well. A buoyancy length-scale, $l_b = B_0^{1/4}/N^{3/4}$, was used for normalizing L_p. This length-scale is proportional to the spreading height of a single-phase plume, i.e., $Z_s \propto B_0^{1/4}/N^{3/4}$. The normalized trough depth, $L_p^* = \frac{L_p}{(B_0^{1/4}/N^{3/4})}$, is shown in Fig. 5c. It is observed that L_p^* increases for a sustaining plume trough and reduces for a collapsing trough; a trend akin to L_p. This is expected since L_p increases with ϕ_v for sustaining plume trough, while l_b remains the same since the buoyancy flux is a constant. For a collapsing plume trough, L_p is equal to Z_s corresponding to that value of ϕ_v. As ϕ_v

increases the spreading height decreases while l_b remains the same, resulting in a decreasing trend for normalized trough depth. An interesting point is that, for a collapsing trough, L_p is same as the spreading height for that particular value of ϕ_v, and therefore in a practical sense the normalization should yield a constant, since the buoyancy length-scale is proportional to the spreading height for a single-phase plume. However, for constant Ri_0 and varying ϕ_v, the presence of particles reduces Z_s and hence L_p, but l_b remains a constant. Thus, we get a decreasing trend in Fig. 5c for a collapsing trough.

The trough radius, R_c is another parameter that is sensitive to changes in ϕ_v. It is defined as the horizontal span of the plume trough below the neutral buoyant layer. The radius, R, varies with z and attains a maximum value near the spreading height, Z_s. This value is called the trough radius, R_c, which has important implications for particle re-entrainment. Sparks et al. [26] and Veitch and Woods [29] reported that if the particles move beyond this radial distance, R_c, then they do not get re-entrained. The experimental values of R_c for varying particle volume fraction is given in Table 3. It is seen that R_c decreases with increase in ϕ_v. This is expected since higher ϕ_v indicates more number of particles in the plume and hence the "particle-fall out" phenomenon is vigorous resulting in weakened radial inertia and hence reduction in the value of R_c. A similar behaviour in R_c was seen for varying ϕ_v at other values of Ri_0.

A forced plume entrains the surrounding fluid as it ascends, thereby creating a flow field directed inwards towards the plume axis. The particles released from the plume and the radial intrusion [18] will be drawn inwards by this flow-field as they fall due to their setting velocity. If the particles are too close to the plume then they can be re-entrained [13, 26]. The particle that does not get re-entrained will fall towards the source. Sparks et al. [26] developed a theoretical formulation for R_c in a homogeneous (unstratified) environment by considering the equations of motions for a sedimenting particles that incorporates the fluid entrainment and particle settling velocity. We extend their model for a stratified environment. The coordinate system used in derivation are shown in Fig. 3 with the origin $(r = 0, z = 0)$ at the source of the plume. The equations of motion for sedimenting particles in a forced plume with background stratification is given by,

$$r\frac{dr}{dt} = bu_e \tag{6}$$

$$\frac{dz}{dt} = \phi_v w_s(z) \tag{7}$$

where u_e is the entrainment velocity, $w_s(z)$ is the settling velocity and $b(z)$ is the plume width. Equation (6) is a result of continuity that accounts for the radial motion of the particle due to the entrainment velocity imposed on it due to the fluid motion [13, 26].

Table 3 Comparison of trough radius, R_c, obtained from experiments, Eq. (20), and Sparks et al. [26]

Run no.	N (s^{-1})	ϕ_v (%)	B_0 (m^4/s^3) $\times 10^{-6}$	R_c (expt) (cm)	R_c (Eq. 20) (cm)	R_c (Eq. 22) (cm)
1	0.67	0.35	5.31	10.26	9.59	6.52
2	0.67	0.45	5.31	9.23	8.01	6.41
3	0.67	0.5	5.31	8.87	7.39	6.35
4	0.67	0.7	5.31	7.60	5.66	6.13

Equation (7) considers the vertical motion of a particle, which here is the settling velocity of the particle. Sparks et al. [26] did not account for the effect of volume fraction in their formulation and considered a constant settling velocity due to unstratified environment. But in our formulation we include ϕ_v to account for particle loading. Additionally, we consider the settling velocity to be a function of z as a result of background stratification imposed in our study. This is because, the density difference between the ambient fluid and the particles is quite large (by a factor of 2.5). Therefore, we account for the buoyancy difference in the particle settling velocity with height, since this may play a significant role. The plume width, $b(z)$ and the entrainment velocity, u_e, are defined based on the entrainment assumption as [20]

$$b = \frac{6\alpha z}{5} \tag{8}$$

$$u_e = \alpha W \tag{9}$$

where $\alpha = 0.068$ is the entrainment coefficient that takes a constant value for a forced plume (see [18]). The time averaged velocity at plume axis, $W(z)$, for a forced plume could be written as [20]:

$$W = 5B_0^{1/3} z^{-1/3} \tag{10}$$

The above equation was derived by Morton [19] for a plume-like flow. As the forced plume evolves, it transitions from a momentum dominated flow to a buoyancy dominated flow. Since the plume trough forms below the spreading layer, it is prudent to assume that buoyancy is important and hence the velocity relation for a plume is valid in this region. This equation for W was also used by Sparks et al. [26] in their study related to hydrothermal forced plumes in an unstratified environment. The term z is some arbitrary height above the origin. Re-arranging (6) with the help of (9)–(11), we arrive at

$$r\frac{dr}{dt} = \frac{6\alpha z}{5}\alpha W = \frac{6\alpha^2 z}{5} W = C_1 z^{2/3} \tag{11}$$

where $C_1 = 6\alpha^2 B_0^{1/3}$. Using (7), Eq. (11) can be re-written as

$$rdr = C_1 z^{2/3} dt = C_1 z^{2/3} \frac{dz}{\phi_v w_s(z)} \tag{12}$$

The formulation for $w_s(z)$ is

$$w_s(z) = \frac{1}{18}\frac{g}{\mu} d_p^2 \left(\rho_p - \rho(z)\right) \tag{13}$$

where, ρ_p is the particle density and $\rho(z)$ is the density of the linearly stratified background. Using the definition of buoyancy frequency, N, $\rho(z)$ can be re-written as

$$\rho(z) = \rho_0 \left(1 - \frac{N^2}{g} z\right) \tag{14}$$

with ρ_0 being the ambient density at $z = 0$. Therefore, $w_s(z)$ can be now be expressed in terms of z, by combining Eqs. (13) and (14) as follows

$$w_s(z) = p + qN^2 z \tag{15}$$

where, p, and q are constants given as,

$$p = \frac{1}{18}\frac{g}{\mu} d_p^2 (\rho_p - \rho_b);\ q = \frac{1}{18}\frac{\rho_b}{\mu} d_p^2 \tag{16}$$

Thus, Eq. (12) becomes,

$$rdr = C_1 z^{2/3} \frac{dz}{p + qN^2 z} = \frac{C_1}{\phi_v p} z^{2/3} \left(1 + \frac{qN^2}{p} z\right)^{-1} dz \tag{17}$$

Owing to the fact that $\frac{qN^2 z}{p} \ll 1$, (17) can be expanded binomially upto O(1) and ignoring all the higher order terms. Thereafter, integrating (17) between limits of r and z we get an expression for the trough radius as follows,

$$\int_0^R rdr = \int_{z_0}^{z} \frac{C_1}{\phi_v p} z^{2/3} \left(1 - \frac{qN^2 z}{p}\right) dz \tag{18}$$

$$R^2 = \frac{C}{\phi_v} \left[\frac{1}{5}(z^{5/3} - z_0^{5/3}) - \frac{1}{8}\lambda N^2 (z^{8/3} - z_0^{8/3})\right] \tag{19}$$

where $C = \frac{6C_1}{p} = 4400\alpha^2 B_0^{1/3}$ and $\lambda = \frac{q}{p}$.

The expression (19) mathematically depicts the structure of the plume umbrella cloud in the presence of particles below the neutral buoyant layer. Interestingly, there is a trough radius, R_c at the spreading height (Z_s) within which the particles will be re-entrained. If the particles go beyond this radial distance, they will settle down at the plume source. The value of R_c is found by substituting $z = Z_s$ in (19),

$$R_c^2 = \frac{C}{\phi_v} \left[\frac{1}{5}\left(Z_s^{5/3} - z_0^{5/3}\right) - \frac{1}{8}\lambda N^2 \left(Z_s^{8/3} - z_0^{8/3}\right)\right] \tag{20}$$

Mirajkar et al. [18] quantified Z_s as,

$$Z_s = \left[c - c_1 \left(\frac{\phi_v w_s}{(B_0 N)^{1/4}}\right)\right] (B_0/N^3)^{1/4} \tag{21}$$

where c and c_1 are empirical constants reported in [18].

The expression for R_c for a particle-laden plume in a homogeneous environment given by Sparks et al. [26] took the form,

$$R_c^2 = \frac{6A}{5w_s} \left[Z_s^{5/3} - z_v^{5/3}\right] \tag{22}$$

where $A = 3.06\alpha^2 B_0^{1/3}$, z_v=height of the plume vent from origin of the axis, and w_s is the constant settling velocity.

The value of R_c obtained from (20) was compared with experiments and is shown in Table 3, where C, λ, and N were calculated based on plume source conditions. A reasonable agreement between the analytical and experimental value is observed with a maximum error within $\pm 10\%$. The reason for this mismatch could be attributed to the approximations used in the model and the accuracy of the image processing technique used

for detecting the edges of a plume. The trough radius, R_c is also calculated from (22) and compared with the corresponding values calculated from (20) showing the importance of new formulation presented here for the particle-laden plume in stratified environment. The formula given in [13, 26] does not match our results since the effect of ϕ_v was not included in their equation.

The effect of Ri_0 on the trough depth, L_p was also studied for a single value of particle volume fraction $\phi_v = 0.5\%$ and the results are shown in Fig. 6. The trough depth increases with decreasing value of Ri_0 irrespective of whether the plume collapses or not. This is because as Ri_0 decreases, the source momentum increases that enables the plume to reach higher vertical distance following which "particle fall-out" and "particle re-entrainment" govern the growth of L_p. For a high momentum flow, the particle re-entrainment is vigorous resulting in higher particle concentration inside the trough. This leads to a larger draw-down of the plume fluid from the neutral buoyant layer causing L_p to increase compared to a low momentum flow. It is also seen from Fig. 6a that for a constant value of ϕ_v, the plume trough does not collapse at higher (lower) values of Ri_0 (W_0). Therefore, if ϕ_v is maintained constant, then the change in the momentum flux could lead to increase or decrease in L_p. The normalized trough depth $L_p^* = \frac{L_p}{(B_0^{1/4}/N^{3/4})}$ as a function of Ri_0 is shown in Fig. 6c. In contrast to the dimensional plot (Fig. 6b), we observe that L_p^* slightly increases and then decreases rapidly with increase in Ri_0. This can be explained using the plume

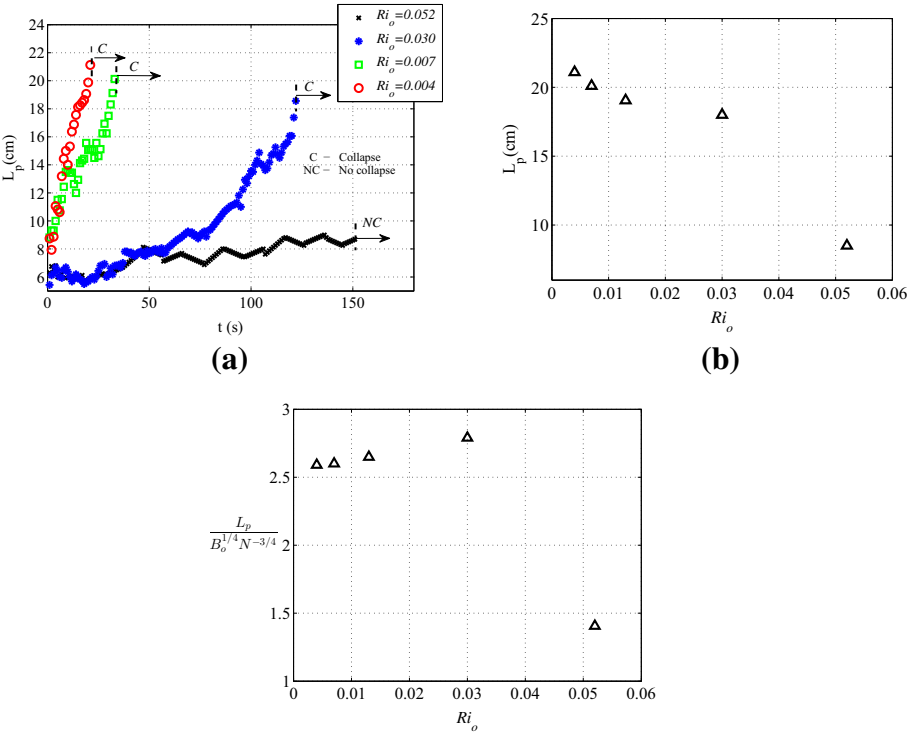

Fig. 6 **a**, **b** Trough depth L_p for different values of source Richardson numbers and fixed $\phi_v = 0.5\%$. **c** Normalized plot of trough depth vs source Richardson number

trough sustenance and collapse. For a constant ϕ_v, at low values of Ri_0, the plume trough collapses for which L_p is equal to Z_s at that particular value of ϕ_v. For a constant value of ϕ_v, as Ri_0 increases, the Z_s of the particle laden plume decreases and hence L_p also decreases. With the increase in Ri_0, the buoyancy flux decreases resulting in a decrease in l_b. Hence, for a collapsing plume trough, any decrease in L_p is offset by a larger decrease in l_b, resulting in an increase in the normalized trough depth, L_p^*. On the other hand, for a sustaining plume trough, L_p is always lower than Z_s, and hence the reduction in L_p is much more than the reduction in l_b and therefore we see a decreasing trend with increasing Ri_0 for a sustaining plume trough.

Experimentally it was seen that with the decrease in Ri_0, the trough radius, R_c, increases, as shown in Fig. 7. Such a trend is observed since the high source momentum of the flow causes the plume to expand radially outward. This increase in R_c at a particular z can also be validated using (20). From (2), as V_0 increases, the source buoyancy flux, B_0 also increases. From (21), as B_0 increases, Z_s increases resulting in a higher value of R_c given by Eq. (20). Generally, Ri_0 can be varied by changing either the volume flow rate, V_0 or the stratification strength N. In the present work, N is same for all experiments and Ri_0 is varied (decreased) by varying (increasing) the volume flow rate, V_0. As V_0 increases, the value of Ri_0 decreases (since M_0 increases at a faster rate than B_0). Therefore, a decrease in Ri_0 leads to an increase in R_c observed from Fig. 7. A similar trend in R_c and L_p were seen for other constant values of ϕ_v. Hence, we only present in detail the results for one such $\phi_v (= 0.5\%)$ and note that the dynamics are same for other values as well. The normalized trough radius, $\frac{R_c}{(B_0^{1/4}/N^{3/4})}$ shows a decreasing trend with increase in Ri_0, which is similar to the dimensional R_c.

4.2 Remark on collapse of the plume trough

Here we focus on the collapse criteria for a particle-laden plume. From the earlier work by Carazzo and Jellinek [6], it is established that a general criteria for plume trough collapse could be formulated based on the effective Richardson number, Ri_0^*. In the experiments by Carazzo and Jellinek [6], the plume behaved more like a fountain where the initial momentum and buoyancy had opposing directions. In the present study, the source momentum and buoyancy have the same sign. For our experiments, it was seen that when

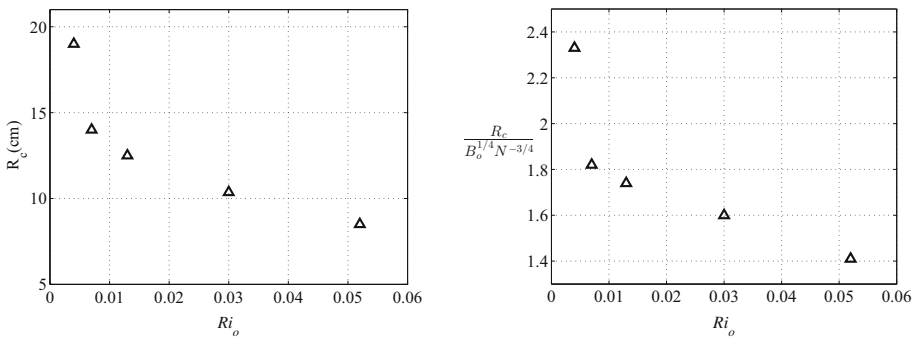

Fig. 7 **a** Variation of trough radius, R_c, with source Richardson's number, Ri_0, **b** normalized plot of trough radius vs source Richardson number

$Ri_0^* < 0.018$, then a particle-laden plume collapses irrespective of ϕ_v and Ri_0. Therefore Ri_0^* is a suitable parameter to qualitatively distinguish between the collapse and stability of a plume trough. From our experiments, we find that a critical value of $Ri_0^* \approx 0.018$ exists that distinguishes the regime of plume trough. Using this critical value of Ri_0^*, for a particular ϕ_v it is possible to get an estimate of W_0 for trough collapse from Equation 5, which could then be used to calculate a critical Ri_0. Doing this, a regime map for sustaining/collapsing trough, as a function of ϕ_v and Ri_0, can be created as shown in Fig. 8. From Fig. 6, at a higher value of $Ri_0 = 0.052$ for $\phi_v = 0.5\%$, the trough did not collapse. Qualitatively, our experiments also revealed that the trough collapsed at $\phi_v = 0.35\%$ when $Ri_0 = 0.007$, while it did not collapse for $Ri_0 = 0.030$. This indicates that as ϕ_v increases, the sustenance of plume trough occurs at a higher value of Ri_0 as illustrated in Fig. 8. Therefore, the plume sustenance/collapse is a strong function of both ϕ_v and Ri_0, and should be accounted for when modeling particle-laden plumes. Our experimental conditions from Table 2 have been overlapped on Fig. 8, which agrees well with the above hypothesis proposed based on the critical value of Ri_0^*.

From the discussion in Sect. 2, it is evident that a combination of ϕ_v and W_0 can give a similar values of Ri_0^*. Therefore, for a given value of Ri_0^*, although the plume may or may not collapse, its trough characteristics depend individually on ϕ_v and Ri_0. The present study gives useful information about the plume trough characteristics and its behaviour, which were missing in earlier studies on this topic (see for e.g. Carazzo and Jellinek [6]).

Our experimental results on positively forced plume with negatively buoyant particles differ from those of Socolofsky and Adams [25], who considered a positively forced plume with positively buoyant particles. Same salient differences are as follows: (a) the structure of plume umbrella cloud is distinctly different in our study compared to than Socolofsky and Adams [25]. This is because, the positively buoyant particles (bubbles/oil droplets) escape from the active recirculation region (below the spreading height), whereas the negatively buoyant particles will be re-circulated and re-entrained in the active region due to their settling velocity. (b) The secondary cloud seen in our experiments is a direct impact of the re-entrainment of particles, which is different from the peeling phenomenon

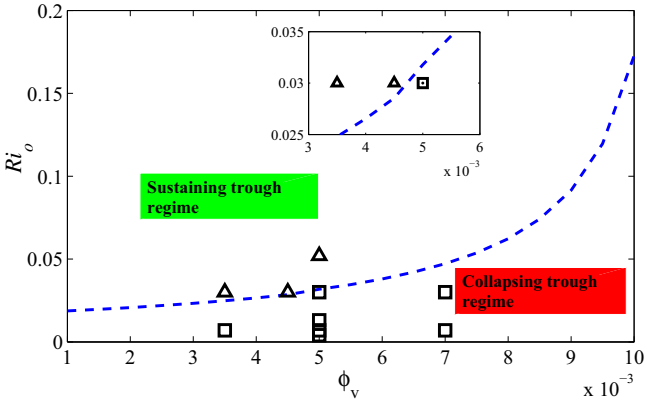

Fig. 8 Regime diagram for plume trough as a function of ϕ_v and Ri_0. The symbol (triangle) correspond to experiments where a sustained plume trough was seen. The symbol box correspond to experiments where plume trough collapsed. The inset (zoom view) shows that the symbols are not touching the dashed line, but are either above or below it. The dashed line corresponds to $Ri_0^* = 0.018$. The symbols represent experimental runs given in Table 2

discussed in Socolofsky and Adams [25]. (c) Lastly, a well-defined trough radius (R_c) and depth (L_p) was measured in our studies, which is not reported in experiments on positively forced plume with positively buoyant particles.

5 Conclusions and application

The effect of dispersed particles on the behaviour of a forced plume was quantified both experimentally and theoretically. When a forced plume with dispersed particles ($\phi_v \leq 1$) grows in time, the particles undergo settling and re-entrainment. Owing to these processes, a distinct plume trough is formed below the primary umbrella cloud, whose structure is characterised by its depth, L_p and trough radius, R_c. Depending on the source conditions, the plume trough either sustains or collapses.

First, the effect of varying ϕ_v on the plume trough characteristics was studied. For a constant value of Ri_0, as ϕ_v increases the value of L_p increases for a sustained plume and decreases for a collapsing plume. This is attributed to the phenomenon of "particle fall-out". The higher value of ϕ_v means more particles in the plume, which have the capacity to drag more fluid downwards and simultaneously reduce the buoyancy. This leads to increased L_p for sustained plumes. On the other hand, for collapsing plumes, $L_p = Z_s$. As ϕ_v increases Z_s decreases [18] and hence L_p also decreases. The trough radius, R_c, decreases with increase in ϕ_v. This is because of vigorous 'particle fall-out' at high values of ϕ_v, which reduces the radial span of the plume trough. A similar trend in L_p and R_c was documented for other constant values of Ri_0 as well. The normalized trough depth, $L_p^* = \frac{L_p}{B_0^{1/4}/N^{3/4}}$, showed a similar trend.

Next, the effect of varying Ri_0 on the plume trough characteristics was studied. For a constant ϕ_v, as Ri_0 decreases the trough radius and depth increases. The increase in the R_c and L_p is due to higher momentum and vigorous "particle re-entrainment" that causes the plume to expand radially and vertically downwards. A similar trend in R_c and L_p was documented for other values of ϕ_v as well. The normalized trough depth, $\frac{L_p}{B_0^{1/4}/N^{3/4}}$ showed a different trend compared to the dimensional plot. For a collapsing plume trough, the decrease in L_p was offset by the reduction in the buoyancy length scale, $l_b = B_0^{1/4}/N^{3/4}$, resulting in an increasing trend in L_p^*. However, for a sustaining plume, L_p^* decreases since the reduction in L_p is more than the reduction in l_b and hence L_p^* decreases with increasing Ri_0 for a sustaining plume trough. The normalized trough radius, $\frac{R_c}{B_0^{1/4}/N^{3/4}}$ had a similar trend to that of dimensional R_c.

In order to qualitatively distinguish the collapsing and sustaining regimes of a particle-laden plume, an effective Richardson number, Ri_0^*, was used. It was experimentally found that when $Ri_0^* < 0.018$, then the plume collapses irrespective of the value of ϕ_v and W_0. Therefore Ri_0^* is a suitable parameter to demarcate the regimes of plume collapse. It should not be used for quantifying the structure (i.e. L_p and R_c) of the plume trough since same value of Ri_0^* can lead to different trough characteristics. From our experiments it was observed that as ϕ_v increases, the value of Ri_0 at which the plume trough sustains also increases. A regime map was created for plume collapse as a function of ϕ_v and Ri_0 and our experimental measurements were in good agreement with this regime map.

An analytical model for the trough radius, R_c, in a stratified environment was developed using a similar approach that was adopted by Sparks et al. [26] for unstratified ambient

conditions. A trough radius, R_c, was formulated from the theoretical model, which explained the re-entrainment dynamics of a particle-laden plume in stratified environment. It was concluded that if a particle stays within this value of R_c, they get re-entrained, otherwise settle on the bottom of the tank. This was also confirmed experimentally and a satisfactory agreement was seen for R_c between experiments and theory.

The experiments on particle-laden plume provide new insight and understanding about the fundamental role of particle settling and re-entrainment on trough formation, plume collapse, and secondary umbrella formation in a stratified environment, which were missing in the past studies. Such process are prevalent in volcanic eruptions and ocean hydrothermal plumes. Although further investigation on the small-scale flow dynamics is needed, the results presented here could be used to model the structure of single-and multi-phase plumes. It was observed that plume collapse was one of the primary reasons leading to the secondary umbrella formation. The concept of particle re-entrainment and collapse has been studied by various researchers [8, 13, 26, 29], but in all these cases it was in an unstratified environment. Therefore, the present work is a significant extension of the meagre studies on this topic. Lastly, the usefulness of this study lies in the fact that it offers new insights about plume trough characteristics, its behaviour with varying ϕ_v and Ri_0, and a regime map for plume trough collapse and sustenance. Such a comprehensive investigation was missing in the earlier studies on this topic.

Acknowledgements SB acknowledges funding from Department of Science and Technology and Ministry of Earth Sciences, India for this research work. HNM is grateful for the research scholarship from IIT Bombay and AKB acknowledges research scholarship from MHRD, India.

References

1. Adalsteinsson D, Camassa R, Harenberg S, Lin Z, McLaughlin R, Mertens K, Reis J, Schlieper W, White B (2011) Subsurface trapping of oil plumes in stratification: laboratory investigations. Geophys Monogr Ser 195:257–262
2. Ai J, Adrian WKL, Yu SCM (2006) On Boussinesq and non-Boussinesq starting forced plumes. J Fluid Mech 558:357–386
3. Balachandar S, Eaton JK (2010) Turbulent dispersed multiphase flow. Annu Rev Fluid Mech 42:111–133
4. Bloomfield L, Kerr R (1998) Turbulent fountains in a stratified fluid. J Fluid Mech 358:335–356
5. Burgisser A, Bergantz G, Breidenthal B (2005) Addressing complexity in laboratory experiments: the scaling of dilute multiphase flows in magmatic systems. J Volcanol Geotherm Res 141(3):245–265
6. Carazzo G, Jellinek A (2012) A new view of the dynamics, stability and longevity of volcanic clouds. Earth Planet Sci Lett 325:39–51
7. Cardoso SS, Mehrãn Z (2001) Sedimentation of polydispersed particles from a turbulent plume. Chem Eng Sci 56(16):4725–4736
8. Carey SN, Sigurdsson H, Sparks RSJ (1988) Experimental studies of particle-laden plumes. J Geophys Res Solid Earth 93:15314–15328
9. Chan GKY (2013) Effects of droplet size on intrusion of sub-surface oil spills. Department of Civil and Environmental Engineering, M.S., Massachusetts Institute of Technology
10. Chow A (2004) Effects of buoyancy source composition on multiphase plume behavior in stratification. Department of Civil and Environmental Engineering, M.S., Massachusetts Institute of Technology
11. Cuthbertson Alan JS, Peter D (2008) Deposition from particle-laden, round, turbulent, horizontal, buoyant jets in stationary and coflowing receiving fluids. J Hydraul Eng 134(4):390–402
12. Ernst G, Sparks R, Carey S, Bursik M (1996) Sedimentation from turbulent jets and plumes. J Geophys Res Solid Earth 101(B3):5575–5589
13. German CR, Sparks RSJ (1993) Particle recycling in the tag hydrothermal plume. Earth Planet Sci Lett 116(1):129–134
14. Hunt G, Kaye N (2005) Lazy plumes. J Fluid Mech 533(3):329–388

15. Jessop D, Jellinek M (2013) The effect of fine particles on ash cloud and plume dynamics. AGU Fall, Meeting Abstracts, p C2860
16. Leah SR (1994) An experimental comparison of bubble and sediment plumes in stratified environments. Master's thesis, Massachusetts Institute of Technology, Civil and Environmental Engineering
17. Mirajkar HN, Balasubramanian S (2017) Effects of varying ambient stratification strengths on the dynamics of a turbulent buoyant plume. J Hydraul Eng 143(04017013):1–10
18. Mirajkar HN, Tirodkar S, Balasubramanian S (2015) Experimental study on growth and spread of dispersed particle-laden plume in a linearly stratified environment. Environ Fluid Mech 15:1241–1262
19. Morton BR (1959) Forced plumes. J Fluid Mech 1:151–163
20. Morton BR, Taylor GI, Turner JS (1956) Turbulent gravitational gonvection from maintained and instantaneous sources. Proc R Soc Lond A 234:1–23
21. Oster G, Yamamoto M (1963) Density gradient techniques. Chem Rev 63:257–268
22. Papanicolaou P, List E (1988) Investigations of round vertical turbulent buoyant jets. J Fluid Mech 195:341–391
23. Richards Tamar S, Aubourg Quentin, Sutherland Bruce R (2014) Radial intrusions from turbulent plumes in uniform stratification. Phys Fluids 26(3):036–602
24. Wang Ruo-Qian, Law Adrian WK, Adams EE, Fringer OB (2011) Large-eddy simulation of starting buoyant jets. Environ Fluid Mech 11(6):591–609
25. Socolofsky SA, Adams EE (2002) Multi-phase plumes in uniform and stratified crossflow. J Hydraul Res 40(6):661–672
26. Sparks R, Carey S, Sigurdsson H (1991) Sedimentation from gravity currents generated by turbulent plumes. Sedimentology 38(5):839–856
27. Sutherland B, Hong Y (2016) Sedimentation from particle-bearing plumes in a stratified ambient. Phys Rev Fluids 1(074302):1–17
28. Turner JS (1986) Turbulent entrainment: the development of the entrainment assumption, and its application to geophysical flows. J Fluid Mech 173:431–471
29. Veitch G, Woods A (2000) Particle recycling and oscillations of volcanic eruption columns. J Geophys Res 105(B2):2829–2842
30. Wang R, Law A, Adams E, Fringer O (2009) Buoyant formation number of a starting buoyant jet. Phys Fluids 21(125104):1–9
31. Wong D, Wright S (1988) Submerged turbulent jets in stagnant linearly stratified fluids. J Hydraul Res 26(2):199–223
32. Woods A (1988) The fluid dynamics and thermodynamics of eruption columns. Bull Volcanol 50(3):169–193